NANO LETTERS

2008
Vol. 8, No. 7
1872-1878

Direct Observation of Atomic Scale Graphitic Layer Growth

Li Liu,[†,§] Kwang Taeg Rim,[†,§] Daejin Eom,[†,‡,§] Tony F. Heinz,[‡,§] and George W. Flynn*[,†,§]

Department of Chemistry, Departments of Physics and Electrical Engineering, The Columbia University Nanoscale Science and Engineering Center, Columbia University, New York, New York 10027

Received February 11, 2008; Revised Manuscript Received May 22, 2008

ABSTRACT

The demand for better understanding of the mechanism of soot formation is driven by the negative environmental and health impact brought about by the burning of fossil fuels. While soot particles accumulate most of their mass from surface reactions, the mechanism for surface growth has so far been characterized primarily by measurements of the kinetics. Here we provide atomic-scale scanning tunneling microscope images of carbon growth by chemistry similar to that of importance in soot formation. At a temperature of 625 K, exposure of the surface of highly ordered pyrolytic graphite to 1 Langmuir of acetylene leads to the formation of both graphitic and amorphous carbonaceous material at the edges of nanoscale pits. Given the similarity of the electronic structure at these graphite defect sites to that of soot material growing in flames at higher temperatures, the present studies shed light on the mechanism for soot growth. These experiments also suggest that healing of defect sites in graphene nanostructures, which are of considerable interest as novel electronic devices, should be possible at modest surface temperatures by exposure of defected graphene to unsaturated hydrocarbons.

The chemistry, structure, and properties of pure carbon materials such as graphite, carbon nanotubes, and single graphite sheets (graphene) are attracting great current attention. This interest is driven by several factors. On the one hand, these materials provide distinctive electrical properties with potential for high-performance electronic devices and sensors. On the other hand, improved understanding of the chemistry of these materials is a central ingredient for control of soot formation during the burning of fossil fuels, a problem with major environmental and health implications.[1] There are at least four consecutive stages in soot growth:[2–4] first, molecular precursors, such as polycyclic aromatic hydrocarbons (PAHs) are formed, typically through homogeneous gas-phase reactions of small aliphatic compounds; second, the PAHs nucleate and further coagulate; third, continued growth of particles occurs through surface-mediated reactions; and finally, particles fuse or agglomerate to form micron-sized soot material. Polyacetylene[5] and ionic species[6] have been proposed as key gaseous species in the early formation and continuous growth of PAHs. Acetylene is also thought to play a significant role in this growth process via the hydrogen-abstraction-C_2H_2-addition (HACA) mechanism.[7] This mechanism has been applied to the surface-reaction stage of soot formation under the assumption that reactions occurring at the surface of soot particles are similar to gaseous reactions taking place at the edges of PAH molecules. Experimental support for this idea is based on the observation that surface growth rates for soot particle formation are proportional to the concentration of C_2H_2 in both laminar premixed[8,9] and diffusion[10] flames.

Recently intense interest has developed in the distinctive charge-transport properties of few-layer or single-layer graphitic sheets (graphene).[11–15] Both for investigations of basic physics and for potential device applications, graphene layers and nanostructures with low defect densities are of central importance. Further, functionalizing such thin layer materials for use in applications remains an intriguing and appealing possibility. Growth of graphitic layers at the edges of carbonaceous seed materials such as PAHs has the potential to open new approaches to the preparation of these materials, which are currently obtained by mechanical exfoliation[11] and thermal decomposition of silicon carbide.[16,17] Much can be learned about the growth, modification, and chemistry of these films by investigating with atomically resolved imaging techniques the chemical behavior of step edges and pits on model, defected highly ordered pyrolytic graphite (HOPG) surfaces exposed to reactive gases. In particular, finding a process to eliminate defects in graphene would be of great value. This capability would permit improvement of existing materials and, importantly, would assist in the fabrication of high-quality patterned graphene nanostructures.[18,19] The chemical behavior of defected graph-

* To whom correspondence should be addressed.
† Department of Chemistry.
‡ Departments of Physics and Electrical Engineering.
§ The Columbia University Nanoscale Science and Engineering Center.

10.1021/nl0804046 CCC: $40.75
Published on Web 06/19/2008

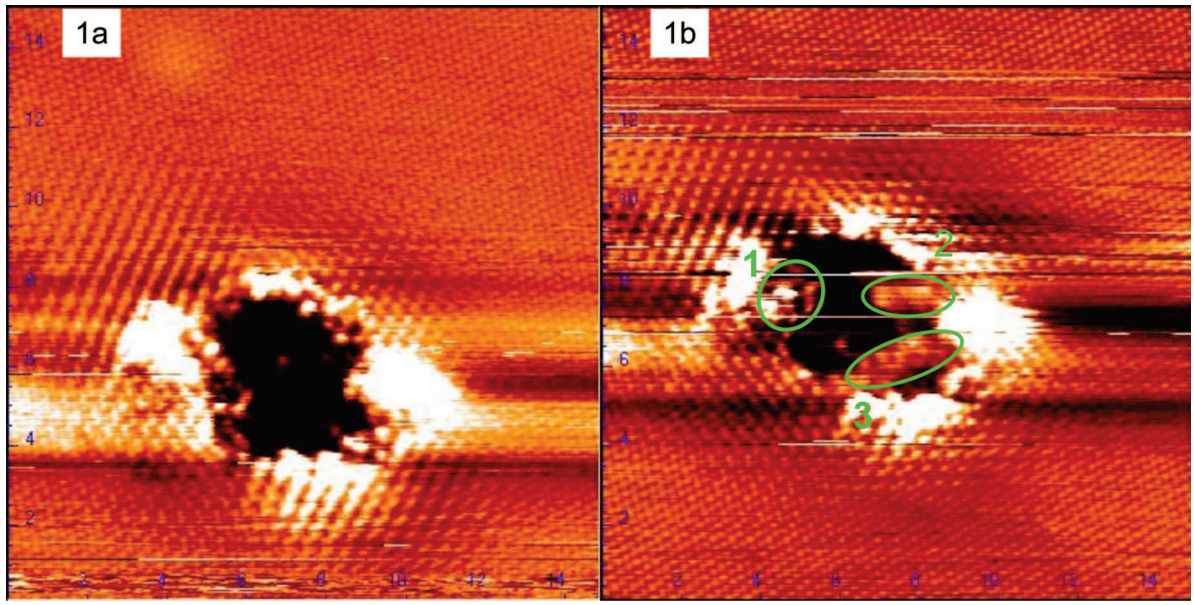

Figure 1. STM images (15 × 15 nm^2) of pit #1 before (a) and after (b) exposure to 1 L of C_2H_2 at 625 K. In (b), three areas changed by this exposure are circled and labeled with numbers.

ite surfaces is likely to mimic reactive processes on single-layer graphene samples, which have recently been imaged by ultrahigh vacuum (UHV) scanning tunneling microscopy (STM).[20,21]

Since its invention some 25 years ago, STM has become a powerful tool to investigate surface structure and dynamics with atomic resolution. This capability is extremely valuable for probing surface reactions. By imaging the same region before and after exposure to reactive species, for example through STM tip engagement techniques,[22] information about reaction mechanisms localized at single atomic surface sites can be extracted. In terms of chemical reactivity, the edges of large PAHs and the surfaces of soot particles in the third stage of growth are analogous to the edges of pits, defect sites and step edges on the highly ordered pyrolytic graphite samples used in the present study. Controlled exposure of these well-characterized, defected HOPG sample surfaces to hydrocarbon fuels such as C_2H_2 under UHV conditions provides an opportunity to investigate the fundamental chemical steps involved in soot formation.

In the present study, HOPG surfaces were prepared with controlled defect sites. This was accomplished by etching procedures through exposure to UV light/ozone treatment and oxygen annealing (see Supporting Information) followed by high-temperature (1050 K) vacuum annealing. STM images were then taken of these model surfaces before and after exposure to acetylene. At moderate surface temperatures (typically 625 K) no change was observed to the undefected part of the graphite surface. At the defect sites, however, reaction with acetylene was found to induce facile growth of both amorphous and ordered carbonaceous material.

An area of the defected HOPG surface with characteristic markers was chosen for study, and the defect pits in this area were imaged first. The tip was then moved away from this focused, characterized area by 300 nm but was kept engaged during this process. Following this initial imaging procedure, the sample was exposed to 1.0 Langmuir of C_2H_2 gas (at a pressure of 1.0×10^{-8} torr). The tip was moved back to the original imaging area 10 min after C_2H_2 exposure, and STM topographs of the same pits were obtained. (The tip is moved away from the imaging area before gas exposure to avoid any surface "shadow effects",[23,24] which could affect the reaction rate for areas of the surface under the tip. Continual engagement on a displaced region of the surface permits the same areas to be reliably imaged both before and after exposure to reactive gas.)

STM images (not shown) recorded on the freshly cleaved, defected, and annealed surface showed carbon (0001) terraces having widths of several hundred nm separated by step edges. Line profile measurements (not shown) of the pits indicated that, in most cases, oxygen reacted with the top graphite layer and left the second layer intact.

Our investigation of the reactivity of these defected surfaces under exposure to actylene was carried out in UHV at a temperture of 625 K. We imaged a 300 × 300 nm^2 area (not shown) that included several pits. This region also included a step edge that served as a useful marker for returning the selected defects after displacement of the STM tip during actylene dosing. Images of four pits in this area were recorded and compared before and after dosing. Two of them (designated as pits #1 and #2 hereafter) showed clear changes.

The initial growth stage of sootlike material is clearly resolved in pit #1 by comparing the images before (Figure 1a) and after (Figure 1b) C_2H_2 exposure. The growth occurred at three areas along the edges of pit #1. While in areas 1 and 2 the new features grow from the edges toward the center of the pit, a bridge forms across the pit in area 3. The $\sqrt{3} \times \sqrt{3}$ R30° superstructure, whose formation has been ascribed to interference between propagating electronic waves and reflected electronic waves near defect edges,[25,26] can be clearly seen around pit #1 in both Figures 1a and 1b.

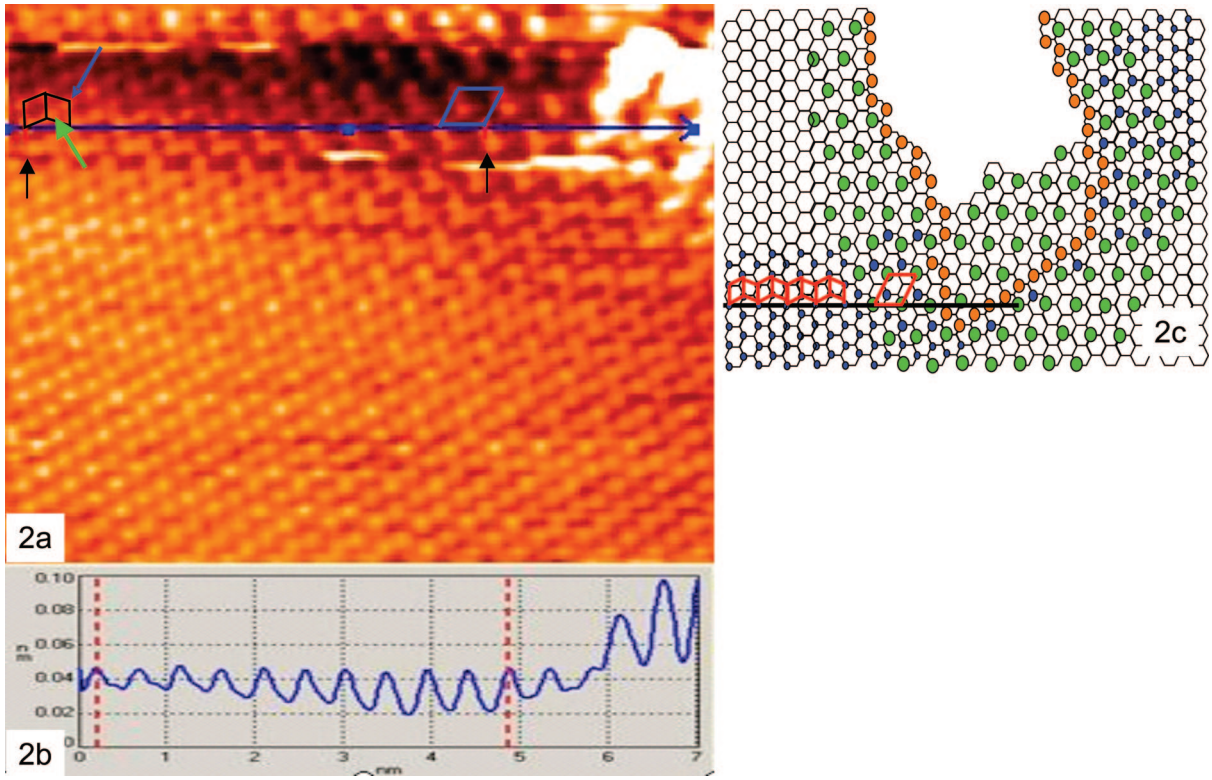

Figure 2. (a) Magnified (7×7 nm^2) STM image of Figure 1b highlights the transition from a graphite hexagonal structure (outlined by the black diamonds) to a $\sqrt{3} \times \sqrt{3}$ R30° superstructure (outlined by the blue diamond). The black arrows indicate the starting and ending points of the line profile shown in (b). The meaning of the blue and green arrows are explained in the text. The model in (c) shows the bridge formed across pit #1 and the transition from hexagonal to superstructure. The blue circles represent the graphite atoms "visible" to the STM tip. Green circles outline the superstructure. Orange circles show the pit edges before C_2H_2 dosing.

The transition from the hexagonally symmetric carbon (0001) structure, normally observed by STM on undefected graphite surfaces, to the $\sqrt{3} \times \sqrt{3}$ R30° superstructure is manifested in Figure 2, obtained by enlarging the bottom left corner of Figure 1b. While the group of atoms indicated by the blue arrow gradually disappears as the scan approaches the pit edge, the group of atoms indicated by the green arrow exhibits an increase in their tunneling probability. The graphite hexagonal structure and the $\sqrt{3} \times \sqrt{3}$ R30° superstructure are shown by the model in Figure 2. Note that the bridge in Figure 3 (enlarged image of area 3 in Figure 1b) displays the same superstructure periodicity (0.445 nm) as the area near the edges (0.447 nm), as is evident from the line profiles. Thus, the newly formed bridge has the graphitic structure.

New features were observed in the lower part of pit #2 and covered about 60% of the pit area. A honeycomb superstructure,[26] which is adjacent to the pit edge, can be seen in an image of the growth area (Figure 4). Line profiles (Figure 5) show that the honeycomb superstructure possesses the same periodicity (0.219 nm) as the hexagonal symmetric carbon (0001) periodicity (0.229 nm) on the graphite surface (the line profile for the graphite surface is not shown). The model in Figure 4 depicts the honeycomb superstructure on a hexagonal symmetric surface. The blue line in the model represents the line profile (Figure 5) through the indicated carbon atoms, and the two green arrows mark the starting and ending points of the distance measured in the line profile. In addition to the honeycomb superstructure, two clumps of carbonaceous material with sizes of ~1 nm × 1 nm wide can be identified. They do not show the carbon (0001) hexagonal periodicity or any of the two superstructure periodicities mentioned above.

On the basis of these results, we can make several observations about the reactivity of solid carbon substrates with the simple hydrocarbon fuel acetylene. First, at least for the modest temperatures (625 K) used here, there is no evidence of reactivity with surface sites other than defects or step edges. This reflects the stability of the delocalized π-bonded graphite sheet structure and the corresponding high barrier to attack by the stable-gas phase reagents. The possibility that acetylene breaks up upon impact and the fragments (e.g., C_2H) diffuse to the reactive edge sites cannot be ruled out by the present data; however such radical species would be expected to react with even the stable delocalized π-bonded graphite sheet structure, a feature that is not observed in the images.

Second, defect sites are clearly more reactive; 2 of 4 investigated defects exhibited carbonaceous growth even for these mild reaction conditions ($T = 625$ K) and modest C_2H_2 exposure times. The low reactivity of graphite compared to soot is well documented, and the present results suggest that at least one reason for this is the paucity of reactive surface sites on typical graphite samples. Indeed, the ability of STM methods to probe a single "interesting" (i.e., reactive) site in the midst of a plethora of unreactive sites is one of the

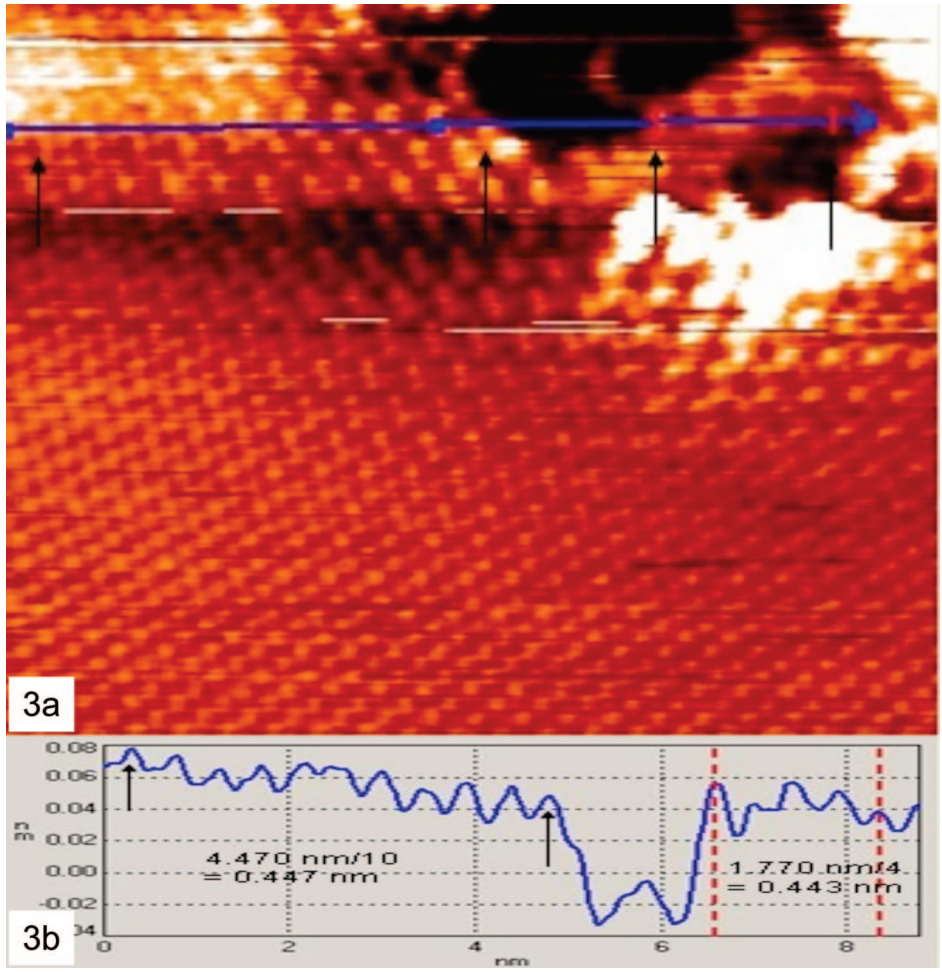

Figure 3. (a) Magnified (9×9 nm^2) STM image of area 3 in Figure 1b. The line profile in 3b shows that the newly formed bridge has the same periodicity as the superstructure at the pit edges. The black arrows indicate the starting and ending points from which the periodicities were calculated.

great advantages of the technique. Nevertheless, to the extent that the electronic structure around graphite defect sites mimics the electronic structure of traditional soot material, graphite reactivity can serve as an excellent model system for unraveling the mechanisms of soot growth. Third, there is clear evidence for the growth of both amorphous and graphitic material at defect sites due to reaction with acetylene (see, e.g., Figures 1, 3, and 4). An interesting question for further study is whether graphite can be cleanly annealed to remove defects by a suitable combination of different hydrocarbon fuels or reaction conditions. Such a procedure could be of great value in producing large scale single graphite (graphene) sheets for use in two-dimensional electronic device applications and for optimizing nanostructures prepared from these materials. From a standpoint of soot formation mechanisms, it will be important to see whether both amorphous and ordered graphitic structures are observed at higher temperatures and with different fuel mixes.

Heicklen et al. have studied the formation of soot material and PAHs in the temperature range 570 to 820 K by pyrolyzing alkynes (acetylene and vinylacetylene) at partial pressures of ~10 torr.[27] The mechanism for this process was identified as homogeneous radical reactions. In the present experiments where C_2H_2 molecules were leaked into the UHV chamber at room temperature, collisions with the hot graphite surface would be required to produce an activated species (C_2H_2*), which in turn could collide with another gas phase molecule to produce, e.g., a radical such as C_2H. Such a radical might undergo further (reactive) collisions with the surface. However, given the low pressure of acetylene employed in the present experiments (10^{-8} torr) such a scenario is highly unlikely. Radical attack of the graphite surface from the gas phase can also be expected to produce chemistry on the smooth (undefected) graphite planes, which is not observed in the current experiments.

Surface reactions can take place through either the Eley−Rideal or the Langmuir−Hinshelwood mechanisms.[28] In the Eley−Rideal mechanism, gas phase reactants collide with reactive surface sites and undergo chemical reactions without equilibrating with the surface. Since the total dosage of C_2H_2 is 1.0 L in the present experiments, each atomic surface site, on average, has the chance to collide with one C_2H_2 molecule during the entire dose time. If the surface reactions take place through the Eley−Rideal mechanism, carbonaceous species would only cover the initial pit edges. However, the experimental results show that the carbonaceous materials cover significant regions of the pit area

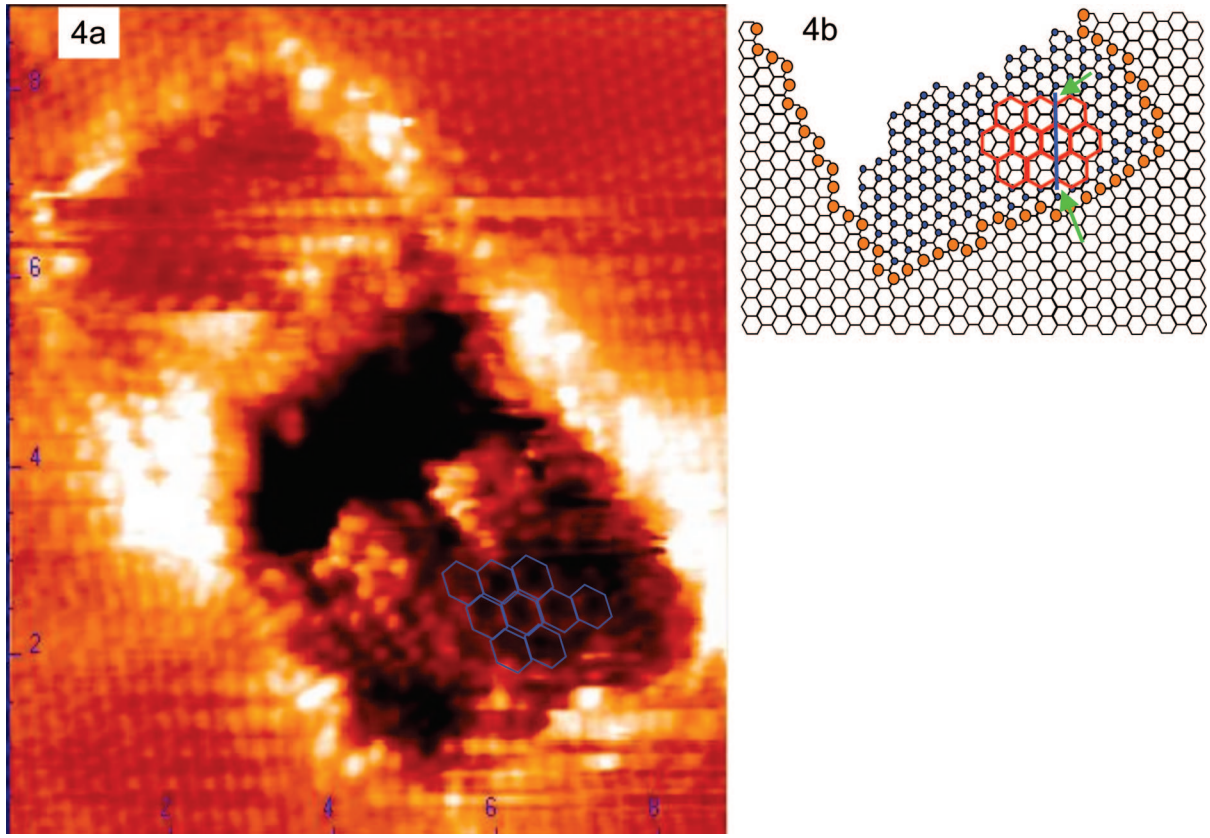

Figure 4. (a) STM images (8.7 × 8.7 nm^2) of the reacted area in pit #2. The honeycomb superstructure is outlined by blue hexagons. The model in panel b highlights the superstructure. The blue circles represent the graphite atoms "visible" to the STM tip. The red hexagons represent the superstructure. The blue line shows how the line profile, presented in Figure 5, was obtained. The green arrows indicate the starting and ending points of the line profile in Figure 5.

(Figures 3a and 4a). Therefore, surface reactions almost certainly take place through a Langmuir−Hinshelwood mechanism in which carbon is initially captured through physisorption of the incident C_2H_2 molecules. These molecules then diffuse, either on the graphite terraces or within the defect pits, until they desorb or encounter reactive sites. At these sites, as discussed below, reactions lead to the formation of the observed carbonaceous material. On the basis of estimates of the energy barriers for desorption and diffusion of physisorbed acetylene molecules, we expect diffusion over several nanometers to occur (see Supporting Information). This distance is sufficient to explain the quantity of carbonaceous material observed experimentally. In the STM images, we see no evidence of physisorbed acetylene, just as expected given the very short lifetime of the molecules on the surface.

The terminations of step edges and defect sites for oxidized carbonaceous materials have attracted the attention of both experimentalists and theoreticians for many years. Chemical titration,[29,30] temperature-programmed desorption,[31] scanning tunneling microscopy and spectroscopy,[32] as well as quantum-chemistry calculations,[33] suggest that these edges are terminated by hydroxyl and carboxyl functional groups for samples prepared in air. Upon high-temperature annealing in UHV, the oxygen and hydrogen atoms are expected to desorb (at least partially) from the surface in the form of H_2O, CO, and CO_2.[31] Thus, it is likely that the heavily annealed samples investigated in our UHV study have at least some zigzag structural defect sites terminated with unreacted carbenes and/or armchair structures terminated with unreacted carbynes.[33] These highly reactive structures present likely points for further radical initiated reactions with unsaturated hydrocarbons such as C_2H_2, even at the relatively low temperatures employed in the present experiments. It is interesting to speculate whether the absence of carbonaceous material growth observed experimentally for two of the pits might reflect the absence of such "dangling bond" reactive sites.

A hydrogen abstraction, C_2H_2 addition (HACA) mechanism has been proposed for the growth of soot particles at high temperatures in flames.[3,4,34] The HACA mechanism consists of two repetitive steps: a hydrogen atom at the edge of a PAH or soot surface is abstracted by a hydrogen atom in the gas phase, followed by C_2H_2 addition to the radical site generated in the first step. To keep the surface growing, hydrogen atoms must be supplied continuously from the gas phase. In flames hydrogen atoms are available from the thermal dissociation of hydrogen molecules. However, under UHV conditions, there is no source of H atoms and only a vanishingly small amount of H_2 is available from residual background gas in the chamber. Nevertheless, as mentioned above, reactive sites are likely available at the pit edges where addition of C_2H_2 molecules to the edge radical sites is energetically favorable and can initiate the growth of

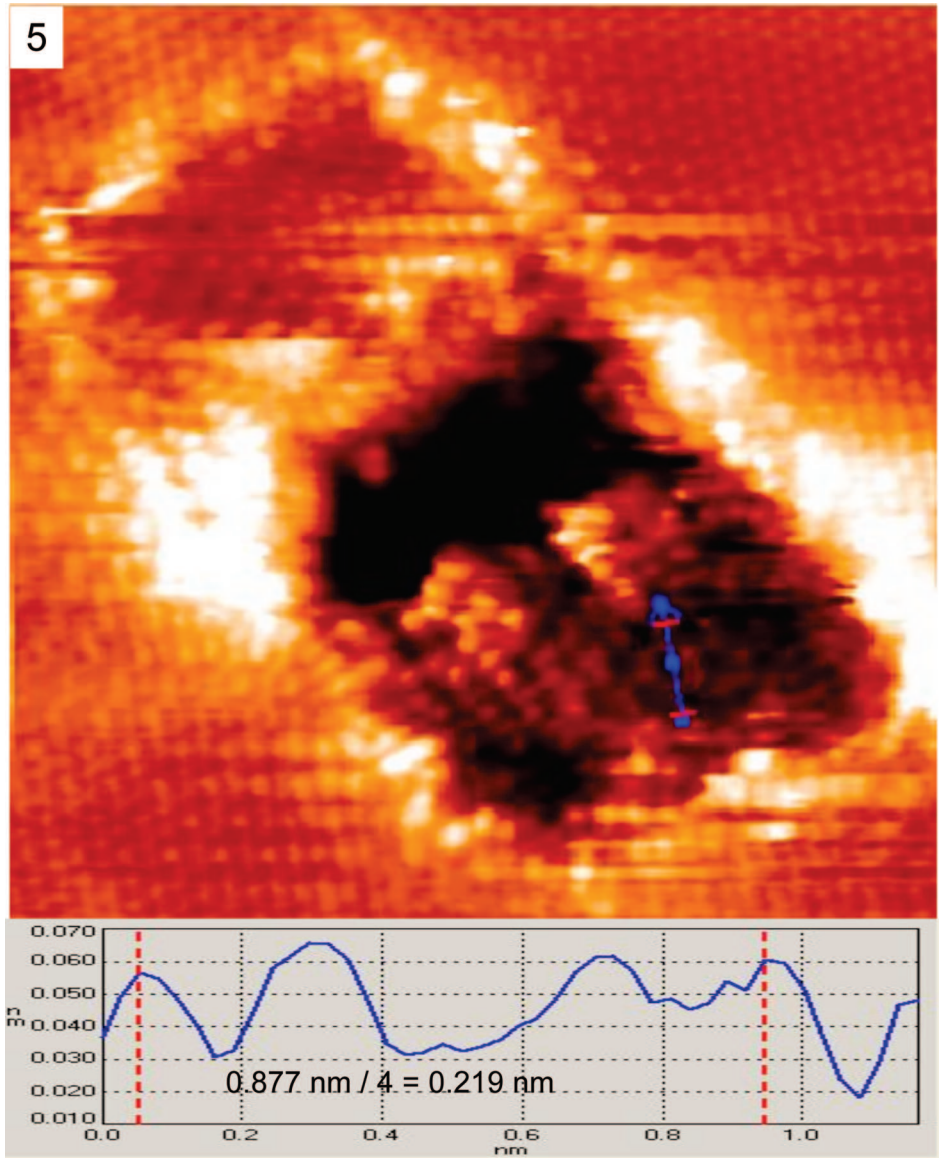

Figure 5. Line profile of the honeycomb superstructure in Figure 4 shows that it has the same periodicity as that of the normal graphite surface.

carbonaceous material. This obviates the necessity for the first step in the HACA mechanism since radical sites are already present from the annealing procedure employed with the UHV sample. However, the growth should have stopped after the edges react with the C_2H_2 molecules if free radicals cannot be supplied continuously at the newly formed edges. Our experimental results show that graphitic structures keep growing until the pits are significantly covered (Figures 3a and 4a).

An adaptation of the HACA mechanism, which could replenish free radical sites at the newly formed armchair edges of the carbonaceous particles as the growth progresses, can be envisioned (reaction 1). First, a C_2H_2 molecule reacts with an existing free radical formed during annealing at one armchair site (step 1), followed by hydrogen atom migration from the aromatic ring to the side chain (step 2). This migration facilitates the direct cyclization between the side chain and the aromatic ring.[35] Finally, the ring closing reaction would need to be accompanied by H_2 molecule release, resulting in a free radical site at the newly formed front edge (step 3). This last step might limit the rate of this reaction given its possibly substantial barrier. In the HACA mechanism, the ring closing reaction is accompanied by H atom release appropriate for growth at the higher temperatures characteristic of combustion flame soot formation.

Besides armchair edges, zigzag edges certainly also exist at the defect and step edge sites. In addition, cyclization at the armchair edges by reaction with C_2H_2 molecules will lead to zigzag edges.[36] A mechanism for the continuous growth of PAHs at zigzag edges has been proposed by Frenklach et al.[34] and references cited therein. This mechanism can be adapted to the present experiments in a manner similar to that described above for the armchair edge mechanism presented in reaction 1.

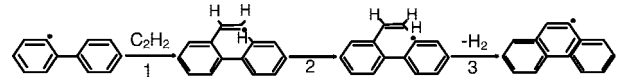

(1)

In summary, growth of carbonaceous material on graphite surfaces has been directly observed using scanning tunneling microscopy. Exposure of deliberately defected graphite samples to acetylene in ultrahigh vacuum at a surface temperature of 625 K results in the formation of both ordered and amorphous new carbon growth. No reaction is observed to take place on smooth graphite surface planes. The low dose of acetylene used in these experiments indicates that the observed growth of new carbon structures proceeds through a mechanism in which initially physisorbed species equilibrate at least partially with the graphite substrate and diffuse on the surface to the defect sites where reaction takes place. Scanning tunneling spectroscopy will be used in the future to determine the nature of the electronic structure of the reactive surface sites both before and after growth of carbonaceous material. Given the similarity of the electronic structure at these graphite defect sites to that of soot material growing in flames at higher temperatures, studies of this type are expected to shed light on the mechanisms for soot growth. In addition these experiments suggest that repair of defect sites in single sheet graphene structures, materials of considerable interest for future electronic devices, may be possible using exposure to unsaturated hydrocarbons at modest surface temperatures.

Acknowledgment. This work was funded by the Department of Energy under Grant DE-FG02-88ER13937 (G.W.F.) and DE-FG02-03ER15463 (T.F.H.). Equipment support was provided by the National Science Foundation under Grant CHE-03-52582 (G.W.F.). We acknowledge financial support from the Nanoscale Science and Engineering Initiative of the National Science Foundation under NSF Award Number CHE-06-41523 and by the New York State Office of Science, Technology, and Academic Research (NYSTAR). The authors are indebted to Michael Frenklach for stimulating discussions regarding the results of this work.

Supporting Information Available: Experimental methods and a calculation of the mean distance diffused by C_2H_2 molecules on the graphite surface at 626 K. This material is available free of charge via the Internet at http://pubs.acs.org.

References

(1) *The Handbook of Environmental Chemistry, Volume 3: Anthropogenic Compounds, Part J: PAHs and Related Compounds: Biology*; Neilson, A. H., Ed.; 1997; p 400.
(2) Harris, S. J.; Weiner, A. M. *Annu. Rev. Phys. Chem.* **1985**, *36*, 31–52.
(3) Richter, H.; Howard, J. B. *Prog. Energy Combust. Sci.* **2000**, *26* (4−6), 565–608.
(4) Frenklach, M. *Phys. Chem. Chem. Phys.* **2002**, *4* (11), 2028–2037.
(5) Homann, K. H.; Wagner, H. G. *Symposium (International) on Combustion, [Proceedings]* **1967**, *11*, 371−378.
(6) Calcote, H. F. *Combust. Flame* **1981**, *42* (3), 215–42.
(7) Frenklach, M.; Wang, H. *Symposium (International) on Combustion, [Proceedings]* **1991**, *23*, 1559–66.
(8) Harris, S. J.; Weiner, A. M. *Combust. Sci. Technol.* **1983**, *32* (5−6), 267–75.
(9) Xu, F.; Sunderland, P. B.; Faeth, G. M. *Combust. Flame* **1997**, *108* (4), 471–493.
(10) Xu, F.; Faeth, G. M. *Combust. Flame* **2001**, *125* (1/2), 804–819.
(11) Novoselov, K. S.; Geim, A. K.; Morozov, S. V.; Jiang, D.; Zhang, Y.; Dubonos, S. V.; Grigorieva, I. V.; Firsov, A. A. *Science* **2004**, *306* (5696), 666–9.
(12) Novoselov, K. S.; Jiang, D.; Schedin, F.; Booth, T. J.; Khotkevich, V. V.; Morozov, S. V.; Geim, A. K. *Proc. Natl. Acad. Sci. U.S.A.* **2005**, *102* (30), 10451–10453.
(13) Zhang, Y.; Tan, Y.-W.; Stormer, H. L.; Kim, P. *Nature (London)* **2005**, *438* (7065), 201–204.
(14) Berger, C.; Song, Z.; Li, X.; Wu, X.; Brown, N.; Naud, C.; Mayou, D.; Li, T.; Hass, J.; Marchenkov, A. N.; Conrad, E. H.; First, P. N.; de Heer, W. A. *Science* **2006**, *312* (5777), 1191–1196.
(15) Ohta, T.; Bostwick, A.; Seyller, T.; Horn, K.; Rotenberg, E. *Science* **2006**, *313* (5789), 951–4.
(16) Forbeaux, I.; Themlin, J. M.; Debever, J. M. *Phys. Rev. B* **1998**, *58* (24), 16396–16406.
(17) Charrier, A.; Coati, A.; Argunova, T.; Thibaudau, F.; Garreau, Y.; Pinchaux, R.; Forbeaux, I.; Debever, J. M.; Sauvage-Simkin, M.; Themlin, J. M. *J. Appl. Phys.* **2002**, *92* (5), 2479–2484.
(18) Han, M. Y.; Oezyilmaz, B.; Zhang, Y.; Kim, P. *Phys. Rev. Lett.* **2007**, *98* (20), 206805/1–206805/4.
(19) Chen, Z.; Lin, Y.-M.; Rooks, M. J.; Avouris, P. *Physica E* **2007**, *40* (2), 228–232.
(20) Stolyarova, E.; Rim, K. T.; Ryu, S.; Maultzsch, J.; Kim, P.; Brus, L. E.; Heinz, T. F.; Hybertsen, M. S.; Flynn, G. W. *Proc. Natl. Acad. Sci. U.S.A.* **2007**, *104* (22), 9209–9212.
(21) Ishigami, M.; Chen, J. H.; Cullen, W. G.; Fuhrer, M. S.; Williams, E. D. *Nano Lett.* **2007**, *7* (6), 1643–1648.
(22) Rim, K. T.; Mueller, T.; Fitts, J. P.; Adib, K.; Camillone, N., III; Osgood, R. M.; Batista, E. R.; Friesner, R. A.; Joyce, S. A.; Flynn, G. W. *J. Phys. Chem. B* **2004**, *108* (43), 16753–16760.
(23) Stipe, B. C.; Rezaei, M. A.; Ho, W. *J. Chem. Phys.* **1997**, *107* (16), 6443–6447.
(24) Dobrin, S.; Harikumar, K. R.; Jones, R. V.; McNab, I. R.; Polanyi, J. C.; Waqar, Z.; Yang, J. *J. Chem. Phys.* **2006**, *125* (13), 133407/1–133407/9.
(25) Mizes, H. A.; Foster, J. S. *Science* **1989**, *244* (4904), 559–562.
(26) Niimi, Y.; Matsui, T.; Kambara, H.; Tagami, K.; Tsukada, M.; Fukuyama, H. *Phys. Rev. B: Condens. Matter* **2006**, *73* (8), 085421/1–085421/8.
(27) Heicklen, J. *Am. Ch. Soc., Div. Fuel Chem., Prepr Pap.* **1987**, *32* (3), 406–16.
(28) Steinfeld, J. I.; Francisco, J. S.; Hase, W. L. *Chemical Kinetics Dynamics*, Second Ed.; Prentice Hall: Englewood Cliffs, NJ, 1999; p 544.
(29) Boehm, H. P.; Diehl, E.; Heck, W.; Sappok, R. *Angew. Chem.* **1964**, *76* (17), 742–51.
(30) Coughlin, R. W.; Ezra, F. S. *Environ. Sci. Technol.* **1968**, *2* (4), 291–7.
(31) Kwon, S.; Vidic, R.; Borguet, E. *Carbon* **2002**, *40* (13), 2351–2358.
(32) Klusek, Z. *Appl. Surf. Sci.* **1998**, *125* (3/4), 339–350.
(33) Radovic Ljubisa, R.; Bockrath, B. *J. Am. Chem. Soc.* **2005**, *127* (16), 5917–27.
(34) Frenklach, M.; Ping, J. *Carbon* **2004**, *42* (7), 1209–1212.
(35) Moriarty, N. W.; Brown, N. J.; Frenklach, M. *J. Phys. Chem. A* **1999**, *103* (35), 7127–7135.
(36) Frenklach, M.; Schuetz, C. A.; Ping, J. *Proc. Combust. Inst.* **2005**, *30* (1), 1389–1396.

NL0804046